Arch Appl Mech
DOI 10.1007/s00419-015-1100-x

SPECIAL

Jianxiang Wang · Liyong Tong · Bhushan L. Karihaloo

A bridging law and its application to the analysis of toughness of carbon nanotube-reinforced composites and pull-out of fibres grafted with nanotubes

Received: 5 June 2015 / Accepted: 20 November 2015

Abstract Bridging laws are essential in predicting the mechanical behaviour of conventional short-fibre-reinforced composites and the emerging nanofibre-reinforced composites. In this paper, we first review some studies on the toughness of carbon nanotube-reinforced composites that is induced by the pull-out of the nanotubes from the matrix, and on the development of the corresponding bridging laws. A close examination of the available bridging laws for carbon nanotubes reveals that some fundamental issues need to be further addressed. We propose a simple nonlinear and smooth bridging law to describe the pull-out force–displacement behaviour of carbon nanotubes from a matrix. This law contains only two material parameters, reflects the basic features of the pull-out experiments, and is easy to use. We then use this bridging law to calculate the fracture toughness of carbon nanotube-reinforced nanocomposites and predict the pull-out force–displacement response of conventional short fibres that are grafted with carbon nanotubes. Some parametric studies are conducted to reveal the influence of various parameters at the nano- and micro-scale on these properties.

Keywords Bridging law · Carbon nanotube composite · Pull-out of fibre · Toughening mechanism

1 Introduction

1.1 Modelling of toughening mechanisms of CNTs in composites

Carbon nanotubes (CNTs) have a high surface-to-volume ratio as well as high strength and stiffness compared with conventional microfibres, so the damage and fracture processes of nanocomposites reinforced by CNTs are inherently and critically governed by the interaction of the matrix and the nanotubes over a large interfacial area. The toughening effects of CNTs in polymers and ceramics are found to be dominated by their bridging and pull-out [1–7], though other toughening mechanisms, such as crack deflection at the CNT/matrix interface, and rupture of CNTs may be present. Therefore, within the framework of continuum mechanics, much research

J. Wang
State Key Laboratory for Turbulence and Complex Systems and Center for Applied Physics and Technology,
Department of Mechanics and Engineering Science, College of Engineering, Peking University, Beijing 100871, China

J. Wang · L. Tong (✉)
School of Aerospace, Mechanical and Mechatronic Engineering, The University of Sydney, Sydney, NSW 2006, Australia
Tel.: +61 2 93516949
Fax: +61 2 93514841
E-mail: liyong.tong@sydney.edu.au

B. L. Karihaloo
School of Engineering, Cardiff University, Cardiff CF24 3AA, UK
E-mail: karihaloob@cardiff.ac.uk

Published online: 31 December 2015

effort has been devoted to quantifying the overall toughness of carbon nanotube-reinforced composites based upon some bridging law, i.e. a relation between the pull-out force and the pull-out displacement of a single nanotube from the matrix.

Fiedler et al. [4] and Wichmann et al. [6] analysed the fracture energy dissipated by pulling out multiple nanotubes from a matrix treating the nanotubes as unidirectional and straight short fibres that are bonded to the matrix by a constant interfacial shear stress, and using the energy consumed by pulling out a single nanotube. Like conventional microfibres, when the embedded length exceeds a critical value, a CNT may break during the opening of a crack, instead of being pulled out. Wichmann et al. [6] also considered the effect of the critical length. This simple analysis clearly shows the effect of some key parameters involved in the pull-out toughening mechanism: the length, radius, and volume fraction of the CNTs, and the interfacial shear strength. They also mentioned another mechanism, namely the work done in the extension of the nanotubes due to their high failure strain (10 % or more). This deformation may not be important for conventional brittle fibres, but it needs to be well examined for CNTs. Tong et al. [8] studied the effect of unidirectional multi-walled CNTs that bridge a crack in a double cantilever beam on the energy release rate of the delamination. Two bridging tractions were considered: the traction caused by the deformation, debonding and pull-out of the CNTs from the substrates, and the pull-out of the inner tube from the outer ones in multi-walled CNTs (the so-called sword-in-sheath pull-out). Upon a detailed examination of the corresponding experimental observations, the former was modelled by a perfectly plastic and frictional pull-out bilinear law, while the latter was modelled by a bilinear bridging law. Chen et al. [9] investigated the optimum combination of the embedded CNT length and the interfacial shear strength for increasing the fracture toughness of CNT-reinforced nanocomposites. The bridging law of the Lawrence shear-lag model [10] for a straight short fibre was used to calculate the increased fracture toughness caused by the bridging traction in the wake of a single mode I crack. The competition of the fibre breakage in the case of strong interfacial bonding and the fibre pull-out in the case of weak bonding gave rise to the optimum combination of these two parameters.

The spatial distribution, orientation, morphology, and interface bonding conditions of CNTs greatly affect the toughening effect. Therefore, many researchers have studied the effect of these factors on the mechanical properties of CNT-reinforced nanocomposites. For example, Seshadri and Saigal [11] calculated the fracture energy induced by the pull-out of bridging nanotubes in a composite. The interface between a CNT and its surrounding matrix was described by a nonlinear shear cohesive model in which the shear force and displacement were related through the Xu–Needleman potential [12,13]. However, they neglected the contribution of the frictional sliding pull-out after the peak force. Seshadri and Saigal [11] also studied the effect of the viscosity of the matrix by performing a viscoelastic analysis. Mirjalili and Hubert [14] modelled the toughening mechanisms of unidirectional and randomly oriented CNTs in CNT-reinforced polymeric composites. They calculated the J-integral for a mode I crack whose wake is bridged by CNTs which can either be pulled out or break if the embedded length is smaller or larger than a critical length. As in the analysis of Wichmann et al. [6], the pull-out of a single CNT was simply governed by a constant interfacial shear stress, which is equivalent to a constant frictional stress along the embedded length of the CNT. For an inclined CNT, the applied tensile stress was transformed into the traction along the CNT by coordinate transformation. Although the J-integral should be calculated over the whole distribution of the orientation angles of the CNTs, in the work of Mirjalili and Hubert [14], the contribution of the randomly oriented CNTs was ignored and counted by a binary zero–one scheme determined by a critical value of orientation. Chen et al. [15] predicted the fracture energy of CNT-reinforced nanocomposites taking into account two vital factors, i.e. the curvature and stochastic failure of CNTs. For the curvature effect, they used a simplified analytical tri-linear bridging law that was developed based on the nonlinear bridging law for curved CNTs established by Chen et al. [16,17]. The original bridging law of Chen et al. [16,17] depicts the complete three-stage deformation of a curved CNT in a matrix, namely the elastic deformation in the bonded stage, the interfacial debonding stage, and the sliding pull-out stage. For the latter, it is assumed that the strength of the CNTs is described by a two-parameter Weibull distribution, where the axial stress is calculated by the formula of Chen et al. [17] for a curved CNT. It is found that the curvature generally decreases the fracture energy. Pavia and Curtin [18] predicted the strength and work of fracture of a nanofibre-reinforced ceramic composite characterized by a single crack bridged by wavy short nanofibres. A bridging law was developed using a shear-lag model of a unit cell, similar to the work of Chen et al. [16,17], following the Lawrence shear-lag model [10]. However, the concept of a virtual pulley of Li et al. [19] was used to simulate the frictional resistance at the exit point of the fibre from the matrix, so the contribution of the friction due to the curvature of the fibre was depicted by an exponential function. The strength of the nanofibre was characterized by a Weibull distribution. The salient finding of Pavia and Curtin

[18] is that there is an optimum combination of the length and radius of curvature of the CNTs which can maximize the strength and toughness of the composite.

The bridging law for a single CNT constitutes the foundation for quantifying the toughening mechanisms of CNT-reinforced nanocomposites. This is similar to the toughening analysis of conventional short-fibre-reinforced composites, for which a wealth of literature has accumulated for various types of materials over the last few decades [20–30]. We analyse below some key bridging laws that are used for the nanocomposites.

1.2 Bridging laws

Although the bonding conditions between a carbon nanotube and a polymer matrix may involve complicated mechanisms [31], it is generally recognized that there is no strong chemical bond without well-designed surface modification, and the CNTs are bonded to polymer matrices (for example, epoxy, polypropylene, polystyrene) through electrostatic interaction, van der Waals interaction, possible discrete covalent bonding, and even mismatch of deformation and coefficients of thermal expansion [32–36]. However, significant higher interfacial bonding strengths than conventional carbon fibre–polymer matrix composites could be obtained [34,35,37], and surface modification can also be used to increase the bonding strength [38]. Due to their high strength and the relatively low interfacial shear strength, CNTs are observed to be pulled out from polymer matrices at crack faces in composites, with or without breakage [39–41], and for multi-walled CNTs (MWCNTs), the inner tube may be pulled out of the outer shell when the latter breaks—the so-called sword-in-sheath mechanism [40,42]. Therefore, to fully utilize the unique advantages of high strength and high surface area of CNTs in strengthening and toughening various matrices it is necessary to understand and quantify the load transfer between a CNT and its surrounding matrix, as well as the pull-out mechanisms.

The deformation of a CNT relative to the matrix under tensile loading is generally regarded to undergo three major stages [1,6,16,17]: (1) bonded stage when the CNT is fully bonded to the matrix during loading, and the CNT is generally assumed to deform elastically with the matrix; (2) debonding stage when a part of the CNT has debonded from the matrix and deforms against the frictional force exerted by the matrix, while the rest of the CNT is still bonded to the matrix; and (3) pull-out stage when the debonding propagates to the entire embedded length of the CNT, but due to friction it is progressively pulled out of the matrix. Although a direct observation of the whole deformation process is difficult, molecular dynamic simulations confirm these three stages of deformation [43–45]. These stages characterize the bridging law in that in the initial stage, the pull-out force increases linearly with the pull-out displacement to a peak load, and then with the propagating interfacial debonding, the force drops steeply as the displacement increases, and finally the force gradually decreases to zero due to the interfacial frictional force. These features are seen in the direct pull-out experimental force–displacement curves [31,35,37]. As indicated by Cooper et al. [35], and also demonstrated by the experiments of Barber et al. [31,37], the pull-out force–displacement curves of CNTs and their ropes from polymer matrices resemble typical pull-out force–displacement curves of microfibres in conventional cementitious and polymer composites, such as polymer fibres from a cement matrix [19,46], glass fibres from polymers [47], carbon fibre z-pins from carbon fibre–epoxy composites [29,48], metallic rods from carbon–epoxy composites [28], and Kevlar threads from a resin [49]. These force–displacement curves are often represented by an idealized simple tri-linear diagram shown in Fig. 1. The tri-linear bridging law and its variations (for example, the simplest variation where stages OA and AB in Fig. 1 are suppressed and only the frictional stage BC is retained) are widely used in predicting constitutive relations and toughness of conventional short-fibre-reinforced composites and CNT-reinforced nanocomposites [15,20,24,26,27,48,50–52].

It should be mentioned that the pull-out length of the CNTs in composites may vary between several hundreds of nanometres and several millimetres [1,4,53], but the length used in the molecular dynamic simulations is much smaller, say only several tens of nanometres [44,45] or even only several nanometres [43,54–56], and the pull-out lengths in the direct experiments of Barber et al. [31,37] are also in the range of several tens of nanometres, relatively small compared to the length in actual composites. Therefore, the actual pull-out displacement corresponding to the stage BC in Fig. 1 should be much larger than that shown here.

Apart from molecular dynamic simulations and limited experiments, models within the framework of continuum mechanics have been developed to calculate various quantities, in particular the stress distribution and interfacial shear strength [57–63]. Here, we only focus on the pull-out bridging law. In this regard, by assuming that the interface between the CNT and the matrix is described by the nonlinear shear cohesive model of Xu and Needleman [12,13], and neglecting the deformation of the CNT but considering the deformation of the matrix, Seshadri and Saigal [11] developed a nonlinear bridging law. Chen et al. [16,17] developed the

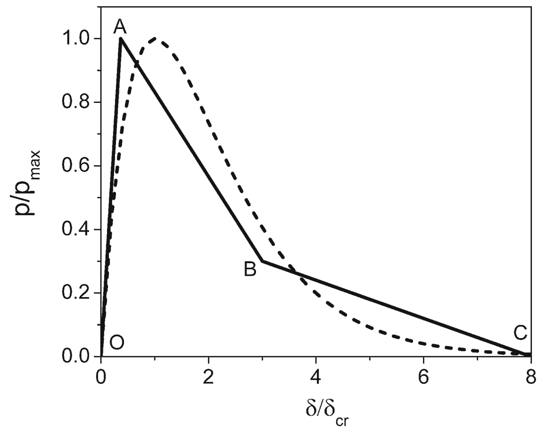

Fig. 1 A tri-linear bridging law (OABC) for pull-out of CNTs and conventional short fibres, where p denotes the pull-out force and δ denotes the pull-out displacement. OA, AB, and BC represent the bonded, debonding, and frictional sliding stages, respectively. p_{max} is the peak force at A. The *dashed line* represents a nonlinear bridging law which is given in Eq. (1)

most comprehensive pull-out model to date that gives a complete pull-out bridging law connecting the three stages of the deformation of the CNT. This model is based on the classical Lawrence shear-lag model [10] for a straight short fibre, but Chen et al. [16,17] made several improvements by taking into account the curvature of the CNT, a nonvanishing force at the embedded end of the CNT that may be caused by entanglement, and a Coulomb friction law in the debonded section. Therefore, the bridging law of Chen at al. [16,17] is a nonlinear and continuous curve that spans the whole range of deformation from the initial elastic deformation to complete pull-out of a curved CNT from a matrix. However, to obtain the curve some numerical computation for a given set of material parameters is necessary. Therefore, to predict the fracture energy of CNT-reinforced nanocomposites, Chen et al. [15] proposed and used a tri-linear bridging law (as shown in Fig. 1) based on their original nonlinear bridging law. They showed that the original nonlinear but complicated bridging law can well be approximated by a tri-linear bridging law. Recently, He et al. [64] presented a pull-out model for an inclined CNT from a matrix. This model takes into account the bending deformation of the CNT and the compressive deformation of the matrix at the exit surface. It can also depict the complete pull-out force–displacement relation, but it also requires some numerical computation. One of the important findings of He et al. [64] is that the predicted maximum pull-out load increases with the inclination angle, similar to the exponential increase given by Li et al. [19].

A close examination of the above bridging laws reveals some issues that need to be further addressed. Firstly, as pointed out by Wang and Karihaloo [65], the problem with the idealized tri-linear bridging law and its variations (Fig. 1) is the discontinuity in the tangent bridging stiffness. The real pull-out curves, both for conventional fibres and CNTs [37,46,49], are nonlinear but smooth, in particular, in the debonding and sliding stages, and for inclined fibres, the abrupt change of the tangent does not comply with the behaviour of real materials. More importantly, with this tri-linear bridging law, it is impossible to model the transition from the strain-hardening to tension-softening, and thus the material instability, of short-fibre-reinforced quasi-brittle and brittle composites. A smooth nonlinear bridging law can also be used to predict the nonlinear behaviour of composites containing multiple micro-cracks [66]. Recently, multiple micro-cracks bridged by boron nitride nanotubes have been found in brittle matrix composites [67]. Secondly, the Lawrence model [10], which has been used to establish the bridging law by Chen et al. [16,17], and also used by Pavia and Curtin [18], is based on the deformation and load transfer of a concentric cylinder where a fibre of a circular cross section is embedded in an outer cylindrical matrix shell. This is probably the most widely used configuration in various shear-lag models since the work of Cox [68]. As a consequence of this configuration, the stresses and displacements given by the shear-lag model will become dependent on a nondimensional parameter $R = \sqrt{\left[1-\left(\frac{r_f}{r_m}\right)^2\left(\frac{E_f}{E_m}\right)\right]}$, where r_f and E_f denote the radius and Young's modulus of the fibre, respectively, E_m denotes Young's modulus of the matrix, and r_m is the outer radius of the matrix shell in the cylindrical shear-lag model. The ratio of r_f/r_m is well defined for an individual cylindrical unit cell, but its definition becomes obscure for a composite material. Cox [68] suggested a way to calculate it by assuming the fibres are arranged hexagonally. Chen et al. [15] used a 'virtual matrix radius' r_m, which is a rather large value. Pavia and Curtin [18] suggested that

$r_f/r_m = \sqrt{V_f}$, by assuming that the volume fraction V_f of the fibre in a composite material can be represented by that in the concentric cylindrical unit cell. It is immediately seen that R will become a complex number when $V_f > V_{fcr} \equiv E_m/E_f$, and so are the displacements and stresses obtained from the shear-lag model. If the typical value $E_f = 1$ TPa is used, then $V_{fcr} \approx 0.3\,\%$ for epoxy [1], and $V_{fcr} = 0.06\,\%$ for polypropylene [69]. The volume fractions of CNTs in composites may range from less than 0.1 % to about 10 % [70]. Therefore, the bridging law based on the concentric cylindrical model may be more applicable for composites with a relatively small value of E_f/E_m so that a large volume fraction of the fibres can be accommodated. Moreover, experiments and simulations [45,53] reveal that CNTs aligned at large oblique angles with respect to the crack surface may break, instead of being pulled out from the matrix, which may reduce the toughening effect. This mechanism has been well studied in conventional composites [23,27]. A combination of a bridging law for CNTs with a proper fibre-discounting scheme may better quantify the toughening effect of CNTs. Apart from the toughening analysis, bridging laws for CNTs may be also applied to the modelling of the pull-out and related properties of carbon fibres grafted with carbon nanotubes [71–73].

Bridging laws of conventional microfibres and the CNTs of the nanoscale have similar features; much can be readily borrowed from the former. Therefore, in this paper, we shall propose a bridging law and attempt to address the issues identified above.

2 An exponential bridging law and determination of the parameters

Although some other models for conventional composites besides those mentioned above can give complete bridging laws [74–77], we want to reduce the numerical computation to the minimum to facilitate their applications, while reflecting the fundamental features of the pull-out processes of both conventional flexible short fibres and CNTs, as well as their composites. To this end, we propose to use the exponential bridging law that has been used by Wang and Karihaloo [65] in their study of material instability in short-fibre-reinforced composites

$$p\,(\delta) = k\delta e^{-\frac{\delta}{\delta_{cr}}} \tag{1}$$

where p denotes the pull-out force and δ denotes the pull-out displacement, respectively; k represents the initial slope (tangent stiffness) of the p–δ curve; and δ_{cr} designates the critical displacement corresponding to the peak of the pull-out force p, where the tangent stiffness vanishes. A comparison of this nonlinear smooth bridging law with the tri-linear bridging law is shown in Fig. 1. The dashed curve of the nonlinear bridging law in Fig. 1 is drawn such that the bridging force is normalized with the peak force, and the initial tangent stiffness k is the same as the slope of the straight line OA. This bridging law is similar to the exponential bridging law developed by Seshadri and Saigal [11] based on the interfacial shear cohesive model of Xu and Needleman [13]

$$p\,(\delta) = k^* \left(\frac{\delta}{\delta_{cr}}\right) e^{-\left(\frac{\delta}{\delta_{cr}}\right)^2} \tag{2}$$

Because the deformation of the CNT is ignored, the parameter k^* of Seshadri and Saigal [11] is related to the fracture energy of the interface and the modulus of the matrix.

With only two parameters k and δ_{cr}, which can be directly measured in an experiment, the bridging law (1) seems to be the simplest. We shall determine these two parameters by considering the deformation mechanisms of CNT-reinforced nanocomposites. First, we determine the initial bridging stiffness k. As mentioned above, the CNTs are bonded to the matrix in the initial stage of deformation, and thus the pull-out displacement is the sum of the elongation of a CNT and the deformation of the matrix. To eliminate the dependence of the deformation of a CNT on the size of the cell in the Lawrence model [10], as mentioned above, we calculate the elongation by letting the outer radius of the cylindrical cell in the Lawrence model approach infinity. In this case, the axial stress in an embedded straight short fibre is a linear function of the distance from the embedded end [10,16,17], and thus the elastic elongation of the CNT under a pull-out force p is simply

$$\delta_{el} = \frac{1}{2}\frac{pl}{E_f A_f} \tag{3}$$

where l denotes the embedded length, and E_f and A_f represent the elastic modulus and cross-sectional area of the CNT, respectively. Fu et al. [78] carried out an analysis of the stress transfer in the pull-out models of a single straight short fibre, and the interaction among multiple fibres. The interaction among multiple fibres will influence the stress transfer of a fibre, but the single-fibre approximation ignoring the interactions is quite accurate for small volume fractions, say $V_{\mathrm{f}} < 5\,\%$, in which case the axial stress in an embedded short fibre is quite accurately depicted by a linear function, as in the Lawrence model [10]. The deformation of the matrix, which is not included in Eq. (3), will be calculated separately. Here, as in the work of Seshadri and Saigal [11], this displacement of the matrix caused by pulling a CNT is approximated by the deformation of a rigid cylindrical indenter of a radius r_{f} imposed on the surface of a semi-infinite medium [79], i.e. the matrix,

$$\delta_{\mathrm{m}} = \frac{1}{2}\frac{1-\nu_{\mathrm{m}}^2}{E_{\mathrm{m}} r_{\mathrm{f}}} p \tag{4}$$

where E_{m} and ν_{m} are the Young modulus and Poisson ratio of the matrix, respectively, and r_{f} is taken as the radius of a CNT. Thus, the total pull-out displacement is

$$\delta = \frac{1}{2}\frac{pl}{E_{\mathrm{f}} A_{\mathrm{f}}}\left[1 + \frac{E_{\mathrm{f}} A_{\mathrm{f}}}{r_{\mathrm{f}} l E_{\mathrm{m}}}\left(1-\nu_{\mathrm{m}}^2\right)\right] \tag{5}$$

A simple analysis for typical CNT-reinforced composites, where $E_{\mathrm{f}} = 1$ TPa, $r_{\mathrm{f}} = 1$ nm, $l = 1\ \mu$m, $E_{\mathrm{m}} = 2$ GPa, and $\nu_{\mathrm{m}} = 0.3$, shows that the second term in the square bracket is in the order of 1 (about 1.4). Therefore, the deformation of the polymer matrix may have the same significance as the deformation of the CNT itself in the initial stage of pull-out. Equation (5) gives the bridging stiffness k in Eq. (1) as

$$k = \frac{2 E_{\mathrm{f}} A_{\mathrm{f}}}{l}\left[1 + \frac{E_{\mathrm{f}} A_{\mathrm{f}}}{r_{\mathrm{f}} l E_{\mathrm{m}}}\left(1-\nu_{\mathrm{m}}^2\right)\right]^{-1} \tag{6}$$

Next, we determine δ_{cr}. For this, the maximum (peak) pull-out force from Eq. (1) is calculated as $p_{\max} = k\delta_{\mathrm{cr}} e^{-1}$. If the peak force, which can be easily measured, is known, then δ_{cr} can be calculated. To keep the calculations to a minimum, and to be consistent with the above analysis, and more importantly, to reflect the experimental and theoretical observations, we calculate the peak force using the formula of Li et al. [19] for the pull-out of an inclined flexible short fibre, that is,

$$p_{\max} = p_0 e^{\mu\varphi} = 2\pi r_f \tau_s l e^{\mu\varphi} \tag{7}$$

where $p_0 = 2\pi r_{\mathrm{f}} \tau_s l$ is the critical pull-out force for a straight fibre of length l and interface shear strength τ_s, and μ is the snubbing friction coefficient for an inclined fibre with an inclination angle φ with the normal direction of the crack surface [19]. With the above formulas, δ_{cr} is given by

$$\delta_{cr} = \frac{2\pi r_f \tau_s l}{k} e^{1+\mu\varphi} \tag{8}$$

The initial bridging stiffness and the critical pull-out displacement have several features. Firstly, the method to obtain k is consistent with the degenerate Lawrence model [10] as well as the theoretical prediction of Fu et al. [78] where a uniform interfacial shear stress and thus a linear axial stress prevail along the embedded length of the fibre. More importantly, Chen et al. [16,17] show that the initial curvature of a curved CNT has a small effect on the initial bridging stiffness; rather, the length has a significant one. Thus, we propose that the initial bridging stiffness k given in Eq. (6) is also applicable to curved CNTs. Secondly, the experiments of Li et al. [19], and Leung and Ybanez [46] for the pull-out tests of initially bent flexible fibres from mortar show that both the peak force and critical pull-out displacement increase with the inclination angle φ. Though Leung and Ybanez [46] emphasize the difference in the pull-out behaviour of initially bent and straight fibres, it is also pointed out that initially bent and straight fibres with negligible flexible stiffness should have similar behaviour. While the increase in the critical pull-out displacement for an inclined fibre from a brittle matrix such as mortar is due to spalling of the matrix at the exit point, the plastic deformation of polymer matrix at the exit point of conventional microfibres and nanoscale CNTs will have a similar effect [44,75]. Finally, the theoretical analysis of He et al. [64] shows that the peak force of a pulled CNT increases with the inclination angle, consistent with the model of Li et al. [19].

3 Toughness

The energy consumed by pulling out a single CNT with the pull-out force–displacement relation (1) is, assuming that the CNT does not break,

$$G_0 = \int_0^l p(\delta)\,\mathrm{d}\delta = k\delta_{\mathrm{cr}}^2 \left\{ 1 - \left[1 + \frac{l}{\delta_{\mathrm{cr}}} \right] e^{-\frac{l}{\delta_{\mathrm{cr}}}} \right\} \tag{9}$$

The exponential bridging law (1) is similar to the interface traction–separation function in the cohesive model of Needleman [12], which decays to zero when $\delta \to \infty$. In calculating the work of separation, Needleman [12] suggested that the upper limit (i.e. l here) of the integral can be chosen such that the value of the integration is about 95 % of that by setting the upper limit to $\delta \to \infty$. However, the value of l in Eq. (9) should be the pull-out length of a CNT. Thus, a problem emerges as how to determine the upper limit of the integral in (9). To resolve this, we conduct an analysis of the order of magnitude of the ratio $l_{\mathrm{cr}}/\delta_{\mathrm{cr}}$, which can be expressed as

$$\frac{l_{\mathrm{cr}}}{\delta_{\mathrm{cr}}} = \frac{2E_{\mathrm{f}}}{\sigma_u} \left[1 + \frac{E_{\mathrm{f}} A_{\mathrm{f}}}{r_{\mathrm{f}} l_{\mathrm{cr}} E_{\mathrm{m}}} \left(1 - \nu_{\mathrm{m}}^2 \right) \right]^{-1} e^{-(1+\mu\varphi)} \tag{10}$$

To toughen a matrix, the embedded length l should be close to or less than the critical length $l_{\mathrm{cr}} \equiv (\sigma_u r_{\mathrm{f}}/2\tau_s)$, which has been used in Eq. (10), where σ_u is the tensile strength of a CNT. Using $E_{\mathrm{f}} = 1\mathrm{TPa}$, $E_{\mathrm{m}} = 2\,\mathrm{GPa}$, $\tau_s = 50\mathrm{MPa}$, $\sigma_u = 30\,\mathrm{GPa}$, and $\mu = 0.6$ (Li et al. [19]; Chen et al. [17]) and $\varphi = \frac{\pi}{2}$ gives $l_{\mathrm{cr}}/\delta_{\mathrm{cr}} = 1.6$, while $l_{\mathrm{cr}}/\delta_{\mathrm{cr}} = 4.25$ for $\varphi = 0$. Therefore, G_0 can also be well approximated by $G_0 = k\delta_{\mathrm{cr}}^2$, since the CNTs at large angles are likely to be discounted, as described below.

With the pull-out energy for a single CNT in (9), we calculate the fracture energy corresponding to the pull-out of randomly orientated CNTs following Li et al. [23]

$$G = \frac{V_{\mathrm{f}}}{\pi r_{\mathrm{f}}^2} \int_{z=0}^{\frac{L}{2}} \left\{ \int_{\varphi=0}^{\arccos\left(\frac{2z}{L}\right)} G_0(l,\varphi)\, U\left[g(z,L,l_{cr})\right] P(\varphi)\,\mathrm{d}\varphi \right\} P(z)\,\mathrm{d}z \tag{11}$$

In the above integral, L denotes the whole length of a CNT, and other functions are [23]

$$l = \frac{L}{2} - \frac{z}{\cos\varphi} \tag{12}$$

$$P(\varphi) = \sin\varphi \tag{13}$$

$$P(z) = \frac{2}{L} \tag{14}$$

$$U(g) = \begin{cases} 1, & g > 0 \\ 0, & g \le 0 \end{cases} \tag{15}$$

where z denotes the distance of the centroid of a fibre from the matrix crack plane and g is defined as [23]

$$g = z - \left(\frac{L}{2} - l_{\mathrm{cr}} e^{-\mu\varphi} \right) \cos\varphi \tag{16}$$

In the above theory, the CNTs whose pull-out force exceeds the rupture force, which is simply $p_{\mathrm{cr}} = 2\pi r_{\mathrm{f}} \tau_s l_{\mathrm{cr}}$, are discounted. This kind of binary discounting scheme depending on the orientation angle is also used in the work of Mirjalili and Hubert [14], but they used a deterministic critical angle $\varphi_{\mathrm{cr}} = 40°$ by an equivalence plan. As pointed out by Chen et al. [15], the strength of CNTs is unlikely to be uniform along the length, nor to be the same from one to the other, so Chen et al. [15] use the two-parameter Weibull distribution to model the strength of CNTs. Discounting CNTs at large orientation angles is highly necessary considering both the stochastic nature of the strength itself and the possible high stress concentration at the exit point [45]. Moreover, even if the strength of a CNT is perfect, the interface bonding between it and the matrix is quite unlikely to be perfect along its length; weak or imperfect interfacial bonding has been regarded as the reason for lower than expected mechanical properties of CNT-reinforced nanocomposites [80,81]. Recently, Lu et al. [82] developed a model to study the pull-out process of a CNT from a matrix where there is a debonding zone at the interface. It is shown that the interfacial defect has a pronounced deleterious effect on the maximum

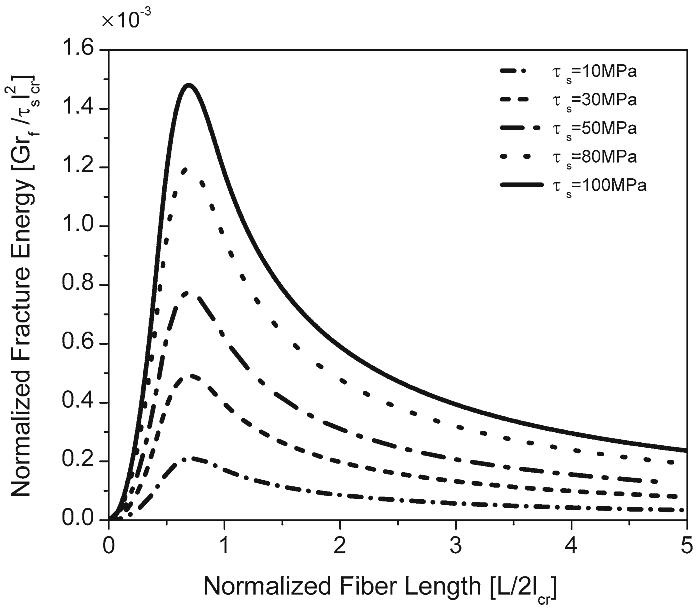

Fig. 2 Variation of normalized fracture energy with normalized length of CNTs. The parameters used are $E_{\mathrm{f}} = 1$ TPa, $E_{\mathrm{m}} = 2$ GPa, $\nu_{\mathrm{m}} = 0.3$, $\sigma_u = 30$ GPa, $\mu = 0.6$, $r_{\mathrm{f}} = 1$ nm, and $V_{\mathrm{f}} = 0.5\,\%$

pull-out force, and the strengthening and toughening effect. Therefore, even for a perfect CNT with a length less than the critical length and aligned perpendicular to the crack face, its strengthening and toughening effect is still likely to be discounted by imperfect interfacial bonding, though the quantification of the effect requires detailed experiments. To reflect all these influences, we replace the binary and deterministic function $U(g)$ in (15) by a smooth degradation function

$$U\,(g) = \frac{1}{2}\,[1 + \tanh\,(Ag)] \tag{17}$$

where the parameter A is a judiciously chosen large positive number depending upon the desired strictness of discounting CNTs. It is easy to verify that such a weighted expression in Eq. (17) can approximate the original (binary) step function in Eq. (15) to any desired accuracy. This continuous and smoothing function was proposed by Wang and Karihaloo [83], and has been used by Wang and Tong [84] for solving interface contact problems.

With all the above formulas, we can conduct numerical calculations and examine the influence of the involved parameters, such as the length and the interfacial shear strength. Figure 2 shows the variation of the normalized fracture energy with normalized length of CNTs. The maximum fracture energy is attained at $L = 1.5l_{\mathrm{cr}}$, after which the fracture energy quickly decreases with the increase in the length of the CNTs.

4 Pull-out of short fibres grafted with carbon nanotubes

Carbon nanotubes have been grafted on to conventional fibres such as carbon fibres and glass fibres to improve the interfacial bonding strength of the latter in polymer matrices [71,72,85–89]. Hung et al. [86] conducted tensile tests of composites containing carbon fibres that are grafted with CNTs on their surfaces, and found an increase in the tensile strength. Based on the observations of the surface of the pull-out holes left by the carbon fibres in the matrix, Hung et al. [86] proposed three types of deformation of CNTs during the pull-out process: (i) the CNTs break at the CNT/carbon fibre joint; (ii) the CNTs are pulled out from the matrix; and (iii) the CNTs break at a length from the hole and then are pulled out. For the epoxy matrix composite, Hung et al. [86] observed that some CNTs are indeed pulled out, but type (i) is regarded as the major failure mechanism. However, An et al. [88] conducted pull-out tests of carbon nanotube-grafted carbon fibres from epoxy and demonstrated a 94 % increase in the interfacial shear strength with type (ii) as the prevailing mode. Wang et al. [72] found a 30 % increase in the interfacial shear strength from their micro-droplet tests of CNT-grafted carbon fibres due to deteriorated wettability of the carbon fibre surface, but the grafting force for a single CNT may be very strong, with a detaching force up to 5 μN.

Recently, Jia et al. [73] presented a numerical study of the pull-out of CNT-grafted carbon fibres using the finite element computation. At the micro-scale, the CNTs are assumed to be aligned only in the radial direction of the carbon fibre, and the CNTs are bonded to the matrix by a cohesive model [90] in which the pull-out force and the pull-out displacement relation is described by a polynomial function. Then, at the macro-scale, the force exerted by the CNTs on the carbon fibre was modelled by a nonlinear spring, so that the quantities at the two scales were linked up. Jia et al. [73] conducted a series of parametric studies of the influence of the microscopic parameters such as the interfacial properties of the CNT/matrix and the radius and length of the CNTs on the macroscopic pull-out force and pull-out energy.

In this paper, we will calculate the pull-out force–displacement relation of short fibres grafted with CNTs which will reflect the three deformation modes of the CNTs as found in the experiments of Hung et al. [86] and An et al. [88]. We develop a model based on three conditions. Firstly, the CNTs are randomly orientated on the surface of a fibre. CNTs may be randomly orientated or spread within a certain angle or even aligned in a direction on a micro-scale fibre [86], but the effect of the orientation distribution can be easily included in the model once it is known. Secondly, there is the interaction between the fibre and the matrix, though this interaction is very likely affected by grafting the CNTs [72]. In order to retain this inherent effect, we include this interaction by assuming a constant frictional shear stress at the carbon fibre–matrix interface. Thirdly, we neglect the axial deformation of the fibre and thus equate the pull-out displacement of the fibre itself to the pull-out displacement of the CNTs.

The average force of a single CNT taking into account the effect of the distribution of the embedded length and orientation is

$$\bar{p}\,(\delta) = 2\int_{l=0}^{L^*}\left\{\int_{\varphi=0}^{\pi/2} p\,(\delta; l, \varphi)\, D\,[p, \delta]\, P\,(\varphi)\,\mathrm{d}\varphi\right\} P^*\,(l)\,\mathrm{d}l \tag{18}$$

where the force $p\,(\delta; l, \varphi)$ that a single CNT exerts on the fibre is given in Eq. (1). Here, we assume that the maximum length (also the embedded length extending from the surface of the fibre) of the CNTs is L^*, and that the length of the CNTs is uniformly distributed in the region $[0, L^*]$ so that the probability density function $P^*\,(l) = 1/L^*$. A CNT should be discounted, that is, the force should be set to zero, when either the pull-out force exceeds a critical value p_0, which could be limited by the grafting force or the strength of the CNT itself [72], or the pull-out displacement reaches the embedded length. Thus, in the above equation, $D\,[p, \delta]$ represents a discounting factor

$$D\,[p, \delta] = \begin{cases} 0, & p > p_0 \text{ or } \delta > l \\ 1, & \text{otherwise} \end{cases} \tag{19}$$

Using the smoothing function in (16), $D\,[p, \delta]$ can be expressed by a smooth and continuous function as

$$D\,[p, \delta] = \frac{1}{4}\,[1 + \tanh A\,(p_0 - p)]\,[1 + \tanh A\,(l - \delta)] \tag{20}$$

Then, the total force exerted by all the CNTs on the fibre with an embedded length L_F and radius R_F is

$$F\,(\delta) = 2\pi R_F (L_F - \delta) g_D\, \bar{p}\,(\delta) + 2\pi R_F (L_F - \delta)\tau_F \tag{21}$$

The first term on the right-hand side is the force exerted on the fibre by the grafted CNTs, and the second term the interfacial frictional force. g_D is the grafting density of the CNTs on the fibre surface, which could reach several tens of CNTs per square micrometre (e.g. 36 CNTs/μm^2). Equation (21) gives the complete pull-out force–displacement relation of a micro-scale fibre grafted with CNTs. The simple linear dependence of the force on the embedded length agrees with the experiments of Qian et al. [85] and An et al. [88]. Figure 3 shows the pull-out curve of a CNT-grafted fibre calculated following the above procedure. For the used parameters, the pull-out force is dominated by the action of the CNTs, when the pull-out displacement is less than the maximum length of the CNTs. The frictional force between the fibre and the matrix is negligible compared with the action of the CNTs. Therefore, to enhance the resistance of the fibre to the pull-out, it is crucial to use long CNTs.

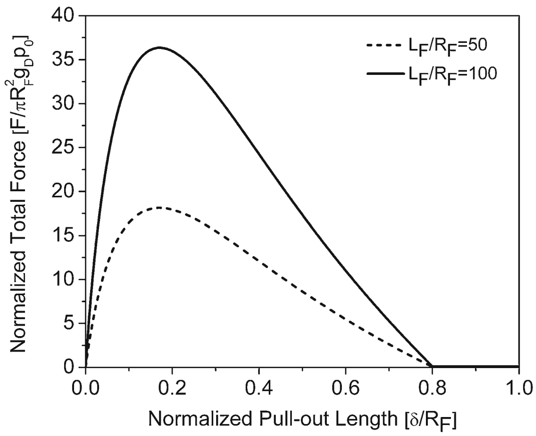

Fig. 3 Pull-out curve of a CNT-grafted fibre. The parameters used are $p_0 = \pi r_{\mathrm{f}}^2 \sigma_u$, $\sigma_u = 70$ GPa, $r_{\mathrm{f}} = 50$ nm, $R_F = 5\,\mu$m, $\tau_F = 10$ GPa, and $L^* = 4\,\mu$m

5 Conclusions

A nonlinear, continuous, and smooth bridging law is proposed to describe the pull-out force–displacement response of carbon nanotubes from a matrix. This bridging law is simple in that it only contains two critical parameters, namely the critical pull-out displacement (or, alternatively, the interface shear strength) and the frictional coefficient for the snubbing effect of inclined CNTs. This bridging law can be used to investigate the strength, constitutive relations, and toughness of carbon nanotube-reinforced nanocomposites when the composites are characterized by cracks bridged by the CNTs. In this paper, it is applied to the prediction of the toughness induced by pull-out of CNTs and to the modelling of the pull-out response of conventional short fibres that are grafted with CNTs on their surfaces. With this simple bridging law, some parametric studies are presented to illustrate the influence of various parameters at the nano- and micro-scale on the toughness of the nanocomposites and the pull-out behaviour of grafted fibres.

Acknowledgments J. Wang and L. Tong thank the support of the China Scholarship Council and the Australian Research Council via Discovery Project Grant (DP130103958). J. Wang also thanks the support of the National Natural Science Foundation of China (Grant Nos. 11232001 and 11521202). Miss Linjuan Wang is thanked for assistance with numerical calculations and figures.

References

1. Gojny, F.H., Wichmann, M.H.G., Kopke, U., Fiedler, B., Schulte, K.: Carbon nanotube-reinforced epoxy-compo sites: enhanced stiffness and fracture toughness at low nanotube content. Compos. Sci. Technol. **64**(15), 2363–2371 (2004)
2. Schulte, K., Gojny, F.H., Wichmann, M.H.G., Fiedler, B.: Influence of different carbon nanotubes on the mechanical properties of epoxy matrix composites—a comparative study. Compos. Sci. Technol. **65**(15–16), 2300–2313 (2005)
3. Xia, Z., Riester, L., Curtin, W.A., Li, H., Sheldon, B.W., Liang, J., Chang, B., Xu, J.M.: Direct observation of toughening mechanisms in carbon nanotube ceramic matrix composites. Acta Mater. **52**(4), 931–944 (2004)
4. Schulte, K., Fiedler, B., Gojny, F.H., Wichmann, M.H.G., Nolte, M.C.M.: Fundamental aspects of nano-reinforced composites. Compos. Sci. Technol. **66**(16), 3115–25 (2006)
5. Cho, J., Inam, F., Reece, M.J., Chlup, Z., Dlouhy, I., Shaffer, M.S.P., Boccaccini, A.R.: Carbon nanotubes: Do they toughen brittle matrices? J. Mater. Sci. **46**(14), 4770–4779 (2011)
6. Wichmann, M.H.G., Schulte, K., Wagner, H.D.: On nanocomposite toughness. Compos. Sci. Technol. **68**(1), 329–331 (2008)
7. Mukhopadhyay, A., Chu, B.T.T., Green, M.L.H., Todd, R.I.: Understanding the mechanical reinforcement of uniformly dispersed multiwalled carbon nanotubes in alumino-borosilicate glass ceramic. Acta Mater. **58**(7), 2685–2697 (2010)
8. Tong, L.Y., Sun, X.N., Tan, P.: Effect of long multi-walled carbon nanotubes on delamination toughness of laminated composites. J. Compos. Mater. **42**(1), 5–23 (2008)
9. Chen, Y.L., Liu, B., He, X.Q., Huang, Y., Hwang, K.C.: Failure analysis and the optimal toughness design of carbon nanotube-reinforced composites. Compos. Sci. Technol. **70**(9), 1360–1367 (2010)
10. Lawrence, P.: Some theoretical considerations of fiber pull-out from an elastic matrix. J. Mater. Sci. **7**(1), 1–6 (1972)
11. Seshadri, M., Saigal, S.: Crack bridging in polymer nanocomposites. J. Eng. Mech. ASCE **133**(8), 911–918 (2007)
12. Needleman, A.: An analysis of tensile decohesion along an interface. J. Mech. Phys. Solids **38**(3), 289–324 (1990)
13. Xu, X.P., Needleman, A.: Numerical simulations of fast crack-growth in brittle solids. J. Mech. Phys. Solids **42**(9), 1397–1434 (1994)

14. Mirjalili, V., Hubert, P.: Modelling of the carbon nanotube bridging effect on the toughening of polymers and experimental verification. Compos. Sci. Technol. **70**(10), 1537–1543 (2010)
15. Chen, X., Beyerlein, I.J., Brinson, L.C.: Bridged crack models for the toughness of composites reinforced with curved nanotubes. J. Mech. Phys. Solids **59**(9), 1938–52 (2011)
16. Chen, X., Beyerlein, I.J., Brinson, L.C.: Curved-fiber pull-out model for nanocomposites. Part 1: bonded stage formulation. Mech. Mater. **41**(3), 279–292 (2009)
17. Chen, X., Beyerlein, I.J., Brinson, L.C.: Curved-fiber pull-out model for nanocomposites. Part 2: interfacial debonding and sliding. Mech. Mater. **41**(3), 293–307 (2009)
18. Pavia, F., Curtin, W.A.: Optimizing strength and toughness of nanofiber-reinforced CMCs. J. Mech. Phys. Solids **60**(9), 1688–1702 (2012)
19. Li, V.C., Wang, Y., Backer, S.: Effect of inclining angle, bundling and surface-treatment on synthetic-fiber pull-out from a cement matrix. Composites **21**(2), 132–140 (1990)
20. Kelly, A.: Interface effects and work of fracture of a fibrous composite. Proc. R. Soc. Lond. Ser. A Math. Phys. Sci. **319**(1536), 95–116 (1970)
21. Marshall, D.B., Cox, B.N., Evans, A.G.: The mechanics of matrix cracking in brittle-matrix fiber composites. Acta Metall. **33**(11), 2013–2021 (1985)
22. Thouless, M.D., Evans, A.G.: Effects of pull-out on the mechanical-properties of ceramic-matrix composites. Acta Metall. **36**(3), 517–522 (1988)
23. Li, V.C., Wang, Y.J., Backer, S.: A micromechanical model of tension-softening and bridging toughening of short random fiber reinforced brittle matrix composites. J. Mech. Phys. Solids **39**(5), 607–625 (1991)
24. Kim, J.K., Mai, Y.W.: High-strength, high fracture-toughness fiber composites with interface control—a review. Compos. Sci. Technol. **41**(4), 333–378 (1991)
25. Jain, L.K., Mai, Y.W.: In the effect of stitching on mode-I delamination toughness of laminated composites. Compos. Sci. Technol. **51**(3), 331–345 (1994)
26. Karihaloo, B.L., Wang, J., Grzybowski, M.: Doubly periodic arrays of bridged cracks and short fibre-reinforced cementitious composites. J. Mech. Phys. Solids **44**(10), 1565–1586 (1996)
27. Fu, S.Y., Lauke, B.: The fibre pull-out energy of misaligned short fibre composites. J. Mater. Sci. **32**(8), 1985–1993 (1997)
28. Cartie, D.D.R., Cox, B.N., Fleck, N.A.: Mechanisms of crack bridging by composite and metallic rods. Compos. Part A Appl. Sci. Manuf. **35**(11), 1325–1336 (2004)
29. Mouritz, A.P., Koh, T.M.: Re-evaluation of mode I bridging traction modelling for z-pinned laminates based on experimental analysis. Compos. Part B Eng. **56**, 797–807 (2014)
30. Wegst, U.G.K., Bai, H., Saiz, E., Tomsia, A.P., Ritchie, R.O.: Bioinspired structural materials. Nat. Mater. **14**(1), 23–36 (2015)
31. Barber, A.H., Cohen, S.R., Kenig, S., Wagner, H.D.: Interfacial fracture energy measurements for multi-walled carbon nanotubes pulled from a polymer matrix. Compos. Sci. Technol. **64**(15), 2283–2289 (2004)
32. Schadler, L.S., Giannaris, S.C., Ajayan, P.M.: Load transfer in carbon nanotube epoxy composites. Appl. Phys. Lett. **73**(26), 3842–3844 (1998)
33. Chang, B.H., Liu, Z.Q., Sun, L.F., Tang, D.S., Zhou, W.Y., Wang, G., Qian, L.X., Xie, S.S., Fen, J.H., Wan, M.X.: Conductivity and magnetic susceptibility of nanotube/polypyrrole nanocomposites. J. Low Temp. Phys. **119**(1–2), 41–48 (2000)
34. Liao, K., Li, S.: Interfacial characteristics of a carbon nanotube-polystyrene composite system. Appl. Phys. Lett. **79**(25), 4225–4227 (2001)
35. Cooper, C.A., Cohen, S.R., Barber, A.H., Wagner, H.D.: Detachment of nanotubes from a polymer matrix. Appl. Phys. Lett. **81**(20), 3873–3875 (2002)
36. Wong, M., Paramsothy, M., Xu, X.J., Ren, Y., Li, S., Liao, K.: Physical interactions at carbon nanotube-polymer interface. Polymer **44**(25), 7757–7764 (2003)
37. Barber, A.H., Cohen, S.R., Wagner, H.D.: Measurement of carbon nanotube-polymer interfacial strength. Appl. Phys. Lett. **82**(23), 4140–4142 (2003)
38. Ding, W., Eitan, A., Fisher, F.T., Chen, X., Dikin, D.A., Andrews, R., Brinson, L.C., Schadler, L.S., Ruoff, R.S.: Direct observation of polymer sheathing in carbon nanotube-polycarbonate composites. Nano Lett. **3**(11), 1593–1597 (2003)
39. Bower, C., Rosen, R., Jin, L., Han, J., Zhou, O.: Deformation of carbon nanotubes in nanotube-polymer composites. Appl. Phys. Lett. **74**(22), 3317–3319 (1999)
40. Qian, D., Dickey, E.C.: In-situ transmission electron microscopy studies of polymer–carbon nanotube composite deformation. J. Microsc. Oxf. **204**, 39–45 (2001)
41. Watts, P.C.P., Hsu, W.K.: Behaviours of embedded carbon nanotubes during film cracking. Nanotechnology **14**(5), L7–L10 (2003)
42. Yu, M.F., Lourie, O., Dyer, M.J., Moloni, K., Kelly, T.F., Ruoff, R.S.: Strength and breaking mechanism of multiwalled carbon nanotubes under tensile load. Science **287**(5453), 637–640 (2000)
43. Frankland, S.J.V., Harik, V.M.: Analysis of carbon nanotube pull-out from a polymer matrix. Surf. Sci. **525**(1–3), L103–L108 (2003)
44. Yang, L., Tong, L., He, X.: MD simulation of carbon nanotube pullout behavior and its use in determining mode i delamination toughness. Comput. Mater. Sci. **55**, 356–364 (2012)
45. Yang, L., Tong, L., He, X., Wagner, H.D., Wang, R.: Molecular dynamic simulation of oblique pullout of carbon nanotube from resin. Comput. Mater. Sci. **83**, 504–12 (2014)
46. Leung, C.K.Y., Ybanez, N.: Pullout of inclined flexible fiber in cementitious composite. J. Eng. Mech. ASCE **123**(3), 239–246 (1997)
47. DiFrancia, C., Ward, T.C., Claus, R.O.: The single-fibre pull-out test. 1. Review and interpretation. Compos. Part A Appl. Sci. Manuf. **27**(8), 597–612 (1996)
48. Dai, S.C., Yan, W.Y., Liu, H.Y., Mai, Y.W.: Experimental study on z-pin bridging law by pullout test. Compos. Sci. Technol. **64**(16), 2451–2457 (2004)

49. Plain, K.P., Tong, L.: Experimental validation of theoretical traction law for inclined through-thickness reinforcement. Compos. Struct. **91**(2), 148–157 (2009)
50. Gopalaratnam, V.S., Shah, S.P.: Tensile failure of steel fiber-reinforced mortar. J. Eng. Mech. ASCE **113**(5), 635–652 (1987)
51. Karihaloo, B.L., Murthy, A.R., Iyer, N.R.: Determination of size-independent specific fracture energy of concrete mixes by the tri-linear model. Cem. Concr. Res. **49**, 82–88 (2013)
52. Bao, G., Suo, Z.: Remarks on crack bridging concepts. Appl. Mech. Rev. **45**, 355–366 (1992)
53. Qian, D., Dickey, E.C., Andrews, R., Rantell, T.: Load transfer and deformation mechanisms in carbon nanotube-polystyrene composites. Appl. Phys. Lett. **76**(20), 2868–2870 (2000)
54. Chowdhury, S.C., Okabe, T.: Computer simulation of carbon nanotube pull-out from polymer by the molecular dynamics method. Compos. Part A Appl. Sci. Manuf. **38**(3), 747–754 (2007)
55. Wernik, J.M., Cornwell-Mott, B.J., Meguid, S.A.: Determination of the interfacial properties of carbon nanotube reinforced polymer composites using atomistic-based continuum model. Int. J. Solids Struct. **49**(13), 1852–1863 (2012)
56. Li, Y., Liu, S., Hu, N., Han, X., Zhou, L., Ning, H., Wu, L., Alamusi, Yamamoto, G., Chang, C., Hashida, T., Atobe, S., Fukunaga, H.: Pull-out simulations of a capped carbon nanotube in carbon nanotube-reinforced nanocomposites. J. Appl. Phys. **113**(14), 144304 (2013)
57. Wagner, H.D.: Nanotube-polymer adhesion: a mechanics approach. Chem. Phys. Lett. **361**(1–2), 57–61 (2002)
58. Lau, K.T.: Interfacial bonding characteristics of nanotube/polymer composites. Chem. Phys. Lett. **370**(3–4), 399–405 (2003)
59. Xiao, K.Q., Zhang, L.C.: The stress transfer efficiency of a single-walled carbon nanotube in epoxy matrix. J. Mater. Sci. **39**(14), 4481–4486 (2004)
60. Xiao, T., Liao, K.: A nonlinear pullout model for unidirectional carbon nanotube-reinforced composites. Compos. Part B Eng. **35**(3), 211–217 (2004)
61. Haque, A., Ramasetty, A.: Theoretical study of stress transfer in carbon nanotube reinforced polymer matrix composites. Compos. Struct. **71**(1), 68–77 (2005)
62. Gao, X.L., Li, K.: A shear-lag model for carbon nanotube-reinforced polymer composites. Int. J. Solids Struct. **42**(5–6), 1649–1667 (2005)
63. Nuriel, S., Katz, A., Wagner, H.D.: Measuring fiber-matrix interfacial adhesion by means of a 'drag-out' micromechanical test. Compos. Part A Appl. Sci. Manuf. **36**(1), 33–37 (2005)
64. He, X., Wang, C., Tong, L., Li, Y., Peng, Q., Mei, L., Wang, R.: A pullout model for inclined carbon nanotube. Mech. Mater. **52**, 28–39 (2012)
65. Wang, J., Karihaloo, B.L.: Material instability in the tensile response of short-fibre-reinforced quasi-brittle composites. Arch. Mech. **52**(4–5), 839–855 (2000)
66. Wang, J.: Overall moduli and constitutive relations of bodies containing multiple bridged microcracks. Int. J. Solids Struct. **39**(8), 2203–2214 (2002)
67. Tatarko, P., Grasso, S., Porwal, H., Chlup, Z., Saggar, R., Dlouhy, I., Reece, M.J.: Boron nitride nanotubes as a reinforcement for brittle matrices. J. Eur. Ceram. Soc. **34**(14), 3339–3349 (2014)
68. Cox, H.L.: The elasticity and strength of paper and other fibrous materials. Br. J. Appl. Phys. **3**(MAR), 72–79 (1952)
69. Dondero, W.E., Gorga, R.E.: Morphological and mechanical properties of carbon nanotube/polymer composites via melt compounding. J. Polym. Sci. Part B Polym. Phys. **44**(5), 864–878 (2006)
70. Thostenson, E.T., Li, C.Y., Chou, T.W.: Nanocomposites in context. Compos. Sci. Technol. **65**(3–4), 491–516 (2005)
71. Thostenson, E.T., Li, W.Z., Wang, D.Z., Ren, Z.F., Chou, T.W.: Carbon nanotube/carbon fiber hybrid multiscale composites. J. Appl. Phys. **91**(9), 6034–6037 (2002)
72. Wang, C., Li, Y., Tong, L., Song, Q., Li, K., Li, J., Peng, Q., He, X., Wang, R., Jiao, W., Du, S.: The role of grafting force and surface wettability in interfacial enhancement of carbon nanotube/carbon fiber hierarchical composites. Carbon **69**, 239–246 (2014)
73. Jia, Y., Chen, Z., Yan, W.: A numerical study on carbon nanotube-hybridized carbon fibre pullout. Compos. Sci. Technol. **91**, 38–44 (2014)
74. Hutchinson, J.W., Jensen, H.M.: Models of fiber debonding and pullout in brittle composites with friction. Mech. Mater. **9**(2), 139–163 (1990)
75. Cox, B.N., Sridhar, N.: A traction law for inclined fiber tows bridging mixed-mode cracks. Mech. Adv. Mater. Struct. **9**(4), 299–331 (2002)
76. Cox, B.N.: Snubbing effects in the pullout of a fibrous rod from a laminate. Mech. Adv. Mater. Struct. **12**(2), 85–98 (2005)
77. Plain, K.P., Tong, L.: Traction law for inclined through-thickness reinforcement using a geometrical approach. Compos. Struct. **88**(4), 558–569 (2009)
78. Fu, S.Y., Yue, C.Y., Hu, X., Mai, Y.W.: Analyses of the micromechanics of stress transfer in single- and multi-fiber pull-out tests. Compos. Sci. Technol. **60**(4), 569–579 (2000)
79. Johnson, K.L.: Contact Mechanics. Cambridge University Press, London (1985)
80. Andrews, R., Weisenberger, M.C.: Carbon nanotube polymer composites. Curr. Opin. Solid State Mater. Sci. **8**(1), 31–37 (2004)
81. Shao, L.H., Luo, R.Y., Bai, S.L., Wang, J.: Prediction of effective moduli of carbon nanotube-reinforced composites with waviness and debonding. Compos. Struct. **87**(3), 274–281 (2009)
82. Lu, Z., Chen, M., Yang, Z.: An improved pull-out model for the carbon nanotube/nanofiber-reinforced polymer composites with interfacial defects. Polym. Compos. (2015). doi:10.1002/pc.23174
83. Wang, J., Karihaloo, B.L.: Optimum in situ strength design of composite laminates.1. In situ strength parameters. J. Compos. Mater. **30**(12), 1314–1337 (1996)
84. Wang, J., Tong, L.: A study of the vibration of delaminated beams using a nonlinear anti-interpenetration constraint model. Compos. Struct. **57**(1–4), 483–488 (2002)
85. Qian, H., Bismarck, A., Greenhalgh, E.S., Kalinka, G., Shaffer, M.S.P.: Hierarchical composites reinforced with carbon nanotube grafted fibers: the potential assessed at the single fiber level. Chem. Mater. **20**(5), 1862–1869 (2008)

86. Hung, K.H., Kuo, W.S., Ko, T.H., Tzeng, S.S., Yan, C.F.: Processing and tensile characterization of composites composed of carbon nanotube-grown carbon fibers. Compos. Part A Appl. Sci. Manuf. **40**(8), 1299–1304 (2009)
87. Godara, A., Gorbatikh, L., Kalinka, G., Warrier, A., Rochez, O., Mezzo, L., Luizi, F., van Vuure, A.W., Lomov, S.V., Verpoest, I.: Interfacial shear strength of a glass fiber/epoxy bonding in composites modified with carbon nanotubes. Compos. Sci. Technol. **70**(9), 1346–1352 (2010)
88. An, F., Lu, C., Li, Y., Guo, J., Lu, X., Lu, H., He, S., Yang, Y.: Preparation and characterization of carbon nanotube-hybridized carbon fiber to reinforce epoxy composite. Mater. Des. **33**, 197–202 (2012)
89. Li, Y., Li, Y., Ding, Y., Peng, Q., Wang, C., Wang, R., Sritharan, T., He, X., Du, S.: Tuning the interfacial property of hierarchical composites by changing the grafting density of carbon nanotube using 1,3-propodiamine. Compos. Sci. Technol. **85**, 36–42 (2013)
90. Chaboche, J.L., Girard, R., Levasseur, P.: On the interface debonding models. Int. J. Damage Mech. **6**(3), 220–257 (1997)